Quantum computation using weak nonlinearities: Robustness against decoherence

Hyunseok Jeong*
Centre for Quantum Computer Technology, Department of Physics, University of Queensland, St Lucia, Queensland 4072, Australia
(Received 5 January 2006; published 26 May 2006)

We investigate decoherence effects in the recently suggested quantum-computation scheme using weak nonlinearities, strong probe coherent fields, detection, and feedforward methods. It is shown that in the weak-nonlinearity-based quantum gates, decoherence in nonlinear media can be made arbitrarily small simply by using arbitrarily strong probe fields, if photon-number-resolving detection is used. On the contrary, we find that homodyne detection with feedforward is not appropriate for this scheme because in this case decoherence rapidly increases as the probe field gets larger.

DOI: 10.1103/PhysRevA.73.052320 PACS number(s): 03.67.Mn, 42.50.Dv, 03.67.Lx

I. INTRODUCTION

Decoherence [1] is one of the main obstacles to the observation of quantum phenomena and the realization of quantum-information processing (QIP). Since it is impossible to perfectly isolate a quantum system from its environment, decoherence effects are more or less unavoidable. Long-term existence of a macroscopic quantum superposition [2] is hindered by the decoherence effects [1,3]. Overcoming the destructive effects of decoherence is the central issue for the realization of large-scale quantum computation (QC). Quantum error-correcting codes and entanglement purification protocols have been developed to overcome the destructive effects of decoherence [4].

Strong nonlinear effects in optical systems, on the other hand, could be very useful for the observation of quantum phenomena [5–7] and the implementation of optical QIP [8]. Since currently available nonlinearities are extremely weak, optical fields need to pass through long nonlinear media for observable realizations of quantum effects. This causes the decoherence effects to be overwhelming so that no quantum effects are actually manifest.

Recently, the idea of using weak cross-Kerr nonlinearities combined with strong coherent fields has been developed by several different authors and applied in various ways [9–19]. The general idea of the weak-nonlinearity-based approach is that the weak strength of a nonlinearity can be compensated by using a strong probe coherent field $|\alpha\rangle$ with a very large amplitude α. In particular, Nemoto and Munro suggested a QC scheme using weak nonlinearities and linear optics [14], which has been further developed by Munro *et al.* [15,16]. They also pointed out [17] that the weak-nonlinearity-based QC [14–16] has merit over the linear optics QC based on Knill *et al.*'s proposal [20] for large-scale quantum computation. However, a rigorous investigation of decoherence effects is essential to verify the validity of the weak-nonlinearity-based QC in a real experiment.

Very recently, it was shown [11] that a generation scheme for macroscopic-superposition states [21] combined with the weak-nonlinearity-based approach [9–14] can *per se* overcome decoherence in a nonlinear medium, i.e., as the amplitude α becomes large, decoherence during the nonlinear interaction *decreases*. In the concluding remarks of Ref. [11], it was naively conjectured that the QC scheme [14–17] could also overcome the decoherence effects in the same way. However, it is unclear whether the weak-nonlinearity-based QC can truly overcome decoherence during the nonlinear interactions in this way with different detection-feedforward strategies [14–17].

In this paper, we investigate decoherence effects in weak-nonlinearity-based QC with homodyne detection [14,15,17] and photon-number-resolving detection [16]. We show that as the initial amplitude of the probe coherent state gets larger, decoherence rapidly *increases* in a two-qubit parity gate with homodyne detection [13–15,17]. On the contrary, we find that as the initial amplitude of the probe coherent state gets larger, decoherence *diminishes* in a two-qubit parity gate with photon-number-resolving detection [16]. In other words, decoherence can be made arbitrarily small in this type of gate simply by increasing the probe field amplitude. We explain that this is due to the difference of the geometric requirements in the phase space. Since the two-qubit parity gate is the key element in weak-nonlinearity-based QC [14–17], our result shows that weak-nonlinearity-based QC can naturally overcome decoherence effects but photon-number-resolving detection is needed for such robustness to decoherence.

II. THE TWO-QUBIT PARITY GATE USING WEAK NONLINEARITIES

It was shown that in conjunction with a strong coherent field, two weak nonlinearities are sufficient to implement a parity gate that entangles two qubits as illustrated in Fig. 1

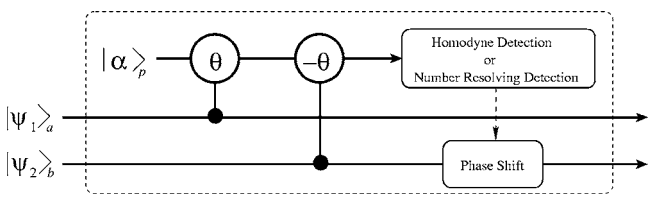

FIG. 1. A schematic of the parity gate using weak nonlinearities that entangles two qubits. The two-mode nonlinear interactions θ and $-\theta$ occur only for the horizontally polarized qubit state $|H\rangle$.

*Electronic address: jeong@physics.uq.edu.au

[13,14]. The interaction Hamiltonian of the cross-Kerr nonlinearity between modes a and p is $H_K=\hbar\chi\hat{a}_a^\dagger\hat{a}_a\hat{a}_p^\dagger\hat{a}_p$, where $\hat{a}$ ($\hat{a}^\dagger$) represents the annihilation (creation) operator and χ is the nonlinear coupling constant. The interaction between a Fock state $|n\rangle_a$ and a probe coherent state $|\alpha\rangle_p$ is described as $U_K(t)|n\rangle_a|\alpha\rangle_p=|n\rangle_a|\alpha e^{in\theta}\rangle_p$, where $\theta=\chi t$ with the interaction time t, and $U_K(t)=e^{iH_Kt/\hbar}$. Using polarization beam splitters, it is possible to use the horizontally and vertically polarized single-photon states $|H\rangle$ and $|V\rangle$ to work as [14] $U_K(t)|H\rangle|\alpha\rangle=|H\rangle|\alpha e^{i\theta}\rangle$ and $U_K(t)|V\rangle|\alpha\rangle=|V\rangle|\alpha\rangle$. For simplicity, we assume two identical initial qubits $|\Psi\rangle_a=(|H\rangle_a+|V\rangle_a)/\sqrt{2}$ and $|\Psi\rangle_b=(|H\rangle_b+|V\rangle_b)/\sqrt{2}$. The total initial state is

$$|\psi_i\rangle=\frac{1}{2}(|H\rangle+|V\rangle)_a(|H\rangle+|V\rangle)_b|\alpha\rangle_p \tag{1}$$

where α is assumed to be real without losing generality. After the first nonlinear interaction between modes a and p with angle θ, the initial state evolves to $|\psi_1\rangle=\{(|HH\rangle+|HV\rangle)_{ab}|\alpha e^{i\theta}\rangle_p+(|VH\rangle+|VV\rangle)_{ab}|\alpha\rangle_p\}/2$. After the second nonlinear interaction between modes b and p with angle $-\theta$, it becomes

$$|\psi_2\rangle=\frac{1}{2}\{(|HH\rangle+|VV\rangle)_{ab}|\alpha\rangle_p+|HV\rangle_{ab}|\alpha e^{i\theta}\rangle_p+|VH\rangle_{ab}|\alpha e^{-i\theta}\rangle_p\}. \tag{2}$$

A measurement is then performed to distinguish the probe beam $|\alpha\rangle_p$ from $|\alpha e^{i\theta}\rangle_p$ and $|\alpha e^{-i\theta}\rangle_p$, while it does not distinguish $|\alpha e^{i\theta}\rangle_p$ and $|\alpha e^{-i\theta}\rangle_p$.

Suppose that homodyne detection for quadrature $\hat{X}=(a+a^\dagger)/2$ is performed with the measurement result X. As can be seen in Fig. 2(a), the distinguishability of the measurement is determined by the distance

$$d_{HD}=\alpha(1-\cos\theta)\approx\frac{\alpha\theta^2}{2} \tag{3}$$

where the approximation has been made under the assumptions of $\theta\ll1$. Munro *et al.* pointed out that the error probability is $P_{err}\approx10^{-4}$ for $d_{HD}=4$ [15]. If d_{HD} is large enough and the measurement outcome is $X>X_{mid}$, where $X_{mid}=\alpha(1+\cos\theta)/2$, the output state is

$$|\psi_f\rangle=\frac{1}{\sqrt{2}}(|HH\rangle+|VV\rangle)_{ab}. \tag{4}$$

On the other hand, if $X<X_{mid}$, the output state is $|\psi_f'\rangle=(e^{i\phi(X)}|HV\rangle+e^{-i\phi(X)}|VH\rangle)_{ab}/\sqrt{2}$, where $\phi(X)=2\alpha\sin\theta(X-\alpha\cos\theta)$. One can transform the state $|\psi_f'\rangle$ to the state $|\psi_f\rangle$ by a simple phase shift for mode b [14,15] based upon the measurement result.

Instead of homodyne detection, photon-number-resolving detection can be used to distinguish the coherent-state elements for mode p as shown in Fig. 2(b) [16]. The displacement operation $D(-\alpha)$ is then applied before photon-number detection is performed. After the displacement operation, the state $|0\rangle$ can be distinguished from $|\alpha(e^{\pm\theta}-1)\rangle$ by photon-number-resolving detection with measurement n_p. The output state (4) is obtained for $n_p=0$. The resulting state for $n_p\neq0$, $(e^{i\phi(n_p)}|HV\rangle+e^{-i\phi(n_p)}|VH\rangle)_{ab}/\sqrt{2}$, can be transformed to the state (4) by a phase shift with the phase factor $\phi(n_p)=n_p\tan^{-1}[\cot(\theta/2)]$. The distance d_{PD} which determines the distinguishability of the measurement is

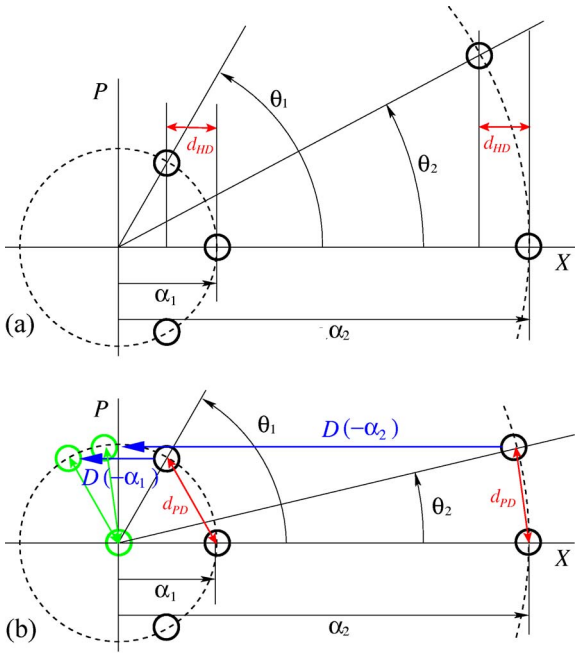

FIG. 2. (Color online) Geometric diagram for the weak-nonlinearity-based two-qubit parity gate using (a) homodyne and (b) photon-number-resolving detection. (a) As the initial amplitude becomes large, the "travel path" $\alpha\theta$ of the coherent state in the phase space should increase to maintain the distance d_{HD}, i.e., $\alpha_2\theta_2>\alpha_1\theta_1$. This causes increase of decoherence effects for large amplitudes. (b) Regardless of the initial amplitude, the travel path $\alpha\theta$ of the coherent state of the same order can maintain the distance d_{PD}, i.e., $\alpha_2\theta_2\approx\alpha_1\theta_1$. This reduces the decoherence effects because the interaction time t in a nonlinear medium becomes shorter as the initial amplitude increases.

$$d_{PD}=2\alpha\sin\frac{\theta}{2}\approx\alpha\theta \tag{5}$$

and the error probability is $P_{err}\approx10^{-4}$ for $d_{PD}=\pi$ [16].

III. DECOHERENCE IN THE WEAK-NONLINEARITY-BASED PARITY GATE

The ideal output state of the two-qubit parity gate should be the pure entangled state (4). However, the actual outcome state will be a mixed state due to the decoherence effects in the nonlinear media. Photon losses may occur both in the probe field mode (p) and in the qubit modes (a and b). However, the possibility of losing photons in the qubit modes becomes lower as the initial amplitude gets larger, because the interaction times ($t=\theta/\chi$) in the nonlinear media become shorter as can be shown from Eqs. (3) and (5). The important factor of decoherence in the two-qubit output state (4) is photon losses in the probe field mode. Since the coherent

field contains a large number of photons, it is easy to lose photons even in a very short time. Such photon losses in the probe coherent field cause the loss of phase information in the two-qubit output state (4). In particular, it is known that a superposition of two distant coherent states rapidly loses its coherence even when it loses a small number of photons [3]. Therefore, photon losses of the probe coherent field in the nonlinear media should be considered the main source of decoherence in the two-qubit output state. In what follows, we shall consider photon losses in the probe field and decoherence effects in the two-qubit output state caused by such photon losses.

Suppose that the probe coherent field loses photons in the first nonlinear medium as $|\alpha\rangle \rightarrow |\mathcal{A}\alpha\rangle$, where we define the amplitude parameter $\mathcal{A}$ (≤ 1). After the first nonlinear interaction, the total initial state becomes a mixed state:

$$\begin{aligned}\frac{1}{4}\{&(|HH\rangle + |HV\rangle)(\langle HH| + \langle HV|) \otimes |\mathcal{A}\alpha e^{i\theta}\rangle\langle \mathcal{A}\alpha e^{i\theta}| \\ &+ \mathcal{C}(|HH\rangle + |HV\rangle)(\langle VH| + \langle VV|) \otimes |\mathcal{A}\alpha e^{i\theta}\rangle\langle \mathcal{A}\alpha| \\ &+ \mathcal{C}^*(|VH\rangle + |VV\rangle)(\langle HH| + \langle HV|) \otimes |\mathcal{A}\alpha\rangle\langle \mathcal{A}\alpha e^{i\theta}| \\ &+ (|VH\rangle + |VV\rangle)(\langle VH| + \langle VV|) \otimes |\mathcal{A}\alpha\rangle\langle \mathcal{A}\alpha|\}_{abp} \qquad (6)\end{aligned}$$

where the coherent parameter $\mathcal{C}$ is introduced to quantify the degree of dephasing. It is easy to recognize that both $\mathcal{A}$ and $\mathcal{C}$ should be reasonably large for the two-qubit parity gate to work properly at the end. If $\mathcal{A}$ is large but $\mathcal{C}$ is negligible, the final output state of the parity gate will be $\rho_f^{(m)} = (|HH\rangle\langle HH| + |VV\rangle\langle VV|)_{ab}/2$, which was also pointed out in Ref. [16]. This completely dephased state $\rho_f^{(m)}$ does not contain entanglement, i.e., the two-qubit parity gate completely fails. On the other hand, if $\mathcal{C}$ is close to 1 but $\mathcal{A}$ is negligible, the final result will be $|\phi_f\rangle = (|H\rangle + |V\rangle)_a(|H\rangle + |V\rangle)_b/2$, which is simply identical to the unentangled initial qubits, so that the gate also fails.

The decoherence effects for a state described by the density operator ρ can be induced by solving the master equation [22]

$$\frac{\partial \rho}{\partial t} = \hat{J}\rho + \hat{L}\rho, \quad \hat{J}\rho = \gamma a \rho a^\dagger, \quad \hat{L}\rho = -\frac{\gamma}{2}(a^\dagger a \rho + \rho a^\dagger a), \qquad (7)$$

where γ is the energy decay rate. The formal solution of the master equation (7) can be written as $\rho(t) = \exp[(\hat{J}+\hat{L})t]\rho(0)$ where t is the interaction time. The evolution of the initial density element $|\alpha\rangle\langle\beta|$ by the decoherence process $\tilde{\mathcal{D}}$ can be described as [22]

$$\tilde{\mathcal{D}}(|\alpha\rangle\langle\beta|) = e^{-(1-e^{-\gamma t})\{(1/2)(|\alpha|^2+|\beta|^2)-\alpha\beta^*\}}|\mathcal{A}\alpha\rangle\langle\mathcal{A}\beta|, \qquad (8)$$

where $|\beta\rangle$ ($|\alpha\rangle$) is a coherent state with amplitude β (α) and $\mathcal{A} = e^{-\gamma t/2}$. However, it should be noted that the decoherence process ($\tilde{\mathcal{D}}$) occurs simultaneously with the unitary evolution ($\tilde{\mathcal{U}}$) by the cross-Kerr interaction Hamiltonian H_K in a nonlinear medium. This combined process can be modeled as follows [11]. One may assume that $\tilde{\mathcal{U}}$ occurs for a short time Δt, and then $\tilde{\mathcal{D}}$ occurs for another Δt. In other words, $\tilde{\mathcal{U}}$ and $\tilde{\mathcal{D}}$ continuously take turns for such short intervals in the nonlinear medium. By taking Δt arbitrarily small, one can obtain an extremely good approximation of this process for a given time t ($=N\Delta t$) with large integer number N. Let us set $\Delta\theta = \chi\Delta t = \pi/N$. In our calculation, we have chosen $N = 10^6$, i.e., $\Delta\theta = \pi/10^6$. This value gives a very good approximation for the whole range of α in our study [11]. Using this model, let us first consider the evolution of one cross term $(|HH\rangle \times \langle VH|)_{ab} \otimes (|\alpha\rangle\langle\alpha|)_p$ in the initial state (1). After time t ($=N\Delta t$) in the nonlinear medium, it evolves to

$$\begin{aligned}&\{\tilde{\mathcal{D}}_p(\Delta t)\tilde{\mathcal{U}}_{ap}(\Delta t)\}^N(|HH\rangle\langle VH|)_{ab} \otimes (|\alpha\rangle\langle\alpha|)_p \\ &\quad = \mathcal{C}(|HH\rangle\langle VH|)_{ab} \otimes (|\mathcal{A}\alpha e^{i\theta}\rangle\langle\mathcal{A}\alpha|)_p \qquad (9)\end{aligned}$$

where $\tilde{\mathcal{U}}(\Delta t)\rho \equiv U_K(\Delta t)\rho U_K^\dagger(\Delta t)$ and

$$\begin{aligned}\mathcal{C} = \exp\Bigg(&-\alpha^2(1-e^{-\gamma(t/N)})\sum_{n=1}^{N}\exp[-\gamma(t/N)]^{(n-1)} \\ &\times\{1-\exp[-i\chi n(t/N)]\}\Bigg). \qquad (10)\end{aligned}$$

The amplitude parameter $\mathcal{A}$ and the coherence parameter $\mathcal{C}$ can then be obtained for an initial amplitude α. We shall use the absolute value of the coherence parameter $|\mathcal{C}|$ to assess the degree of dephasing.

We are interested in $\mathcal{A}$ and $|\mathcal{C}|$ under experimentally realistic assumptions. It is known that an optical fiber of about 3000 km may be required for a nonlinear interaction of $\theta = \pi$ using a currently available cross-Kerr nonlinearity [23]. We first choose $\chi/\gamma = 0.0125$ so that the amplitude will reduce as $\mathcal{A} \approx 0.533$ for 15 km while $\theta = \pi$ is obtained for 3000 km. This corresponds to 0.364 dB/km of signal loss, which is a typical value for commercial fibers used for telecommunication and easily achieved using current technology [24,25]. Note that signal losses in some pure silica core fibers are even less than 0.15 dB/km [25]. Figure 3(a) shows that as the initial amplitude α increases for a fixed d_{HD} (=4), the absolute coherence parameter $|\mathcal{C}|$ (dashed line) rapidly decreases for the homodyne detection scheme. The absolute coherence parameter $|\mathcal{C}|$ is not negligible only when α is small. However, the two-qubit parity gate does not work in this regime because $\mathcal{A}$ (solid line) becomes extremely small. This means the probe coherent state becomes the pure vacuum so that a large $|\mathcal{C}|$ is meaningless. Figure 3(b) shows that this scheme with photon-number detection does not suffer such problems: as the initial amplitude α increases for a fixed d_{PD} ($=\pi$), both $\mathcal{A}$ and $|\mathcal{C}|$ increase for large α. Some detailed values for $\chi/\gamma = 0.0125$ (0.364 dB/km) and $\chi/\gamma = 0.0303$ (0.15 dB/km) including the required length of optical fibers are presented in Table I.

One can understand the difference between Figs. 3(a) and 3(b) by a simple geometric analysis in Fig. 2. For the case of homodyne detection, as the initial amplitude α gets larger, the "travel path" of the coherent state in the phase space, $\alpha\theta$, increases. [Even though θ decreases, the increase of α makes $\alpha\theta$ larger for a fixed d_{HD} ($\approx \alpha\theta^2/2$) as shown in Fig. 2(a).]

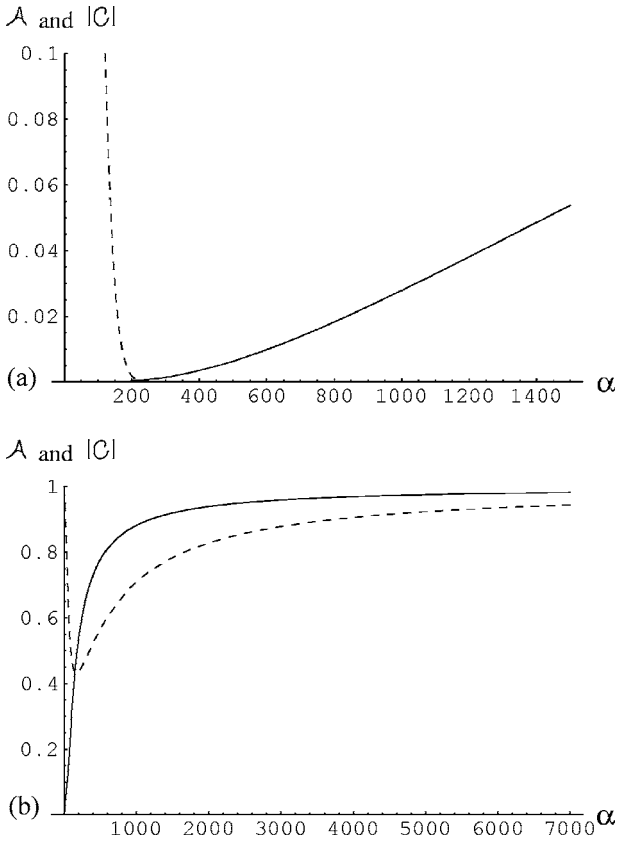

FIG. 3. The amplitude parameter $\mathcal{A}$ (solid line) and the absolute coherence parameter $|\mathcal{C}|$ (dashed line) against the initial amplitude α for homodyne and photon-number detection. The two-qubit parity gate works when both $\mathcal{A}$ and $|\mathcal{C}|$ are large. (a) When homodyne detection is used, it is obvious that the condition of both $\mathcal{A}$ and $|\mathcal{C}|$ being large cannot be met. (b) When photon-number-resolving detection is used, the condition is satisfied for large α.

Therefore, the initial coherent state should travel longer in the phase space. This makes decoherence actually increase as α gets larger. In this case, the principle of increasing α to compensate small θ will not work efficiently. However, the mechanism is totally different when photon-number-resolving detection is used. As the initial amplitude α gets larger, the travel path $\alpha\theta$ does not increase for a fixed d_{PD} ($\approx\alpha\theta$) but remains approximately the same [see Fig. 2(b)]. Therefore, the coherent state travels the same distance regardless of α, while the interaction time t ($=\theta/\chi$), depending on θ, keeps decreasing as α increases. Such decrease of the interaction time t for the same distance causes the decrease of decoherence.

So far, we have considered optical fibers, in which the energy decay rate γ is typically much larger than the nonlinear strength χ as shown in Table I. Munro *et al.* discussed quantum nondemolition (QND) measurements using giant cross-Kerr nonlinearities available in electromagnetically induced transparency (EIT) [12]. This technique can be used to avoid the problems of highly absorptive media. Using this technique, weak-nonlinearity-based QC can be performed in the regime of $\gamma t \approx \chi t\ (=\theta) \ll 1$. This change will certainly improve $\mathcal{A}$ and $|\mathcal{C}|$ for a given value of θ (or a given value of α) in the case of photon-number-resolving detection. For example, if $\chi=0.01$ and $\gamma=0.01$, $\mathcal{A}\approx 0.995$ and $|\mathcal{C}|\approx 0.982$ are obtained for $\theta\approx 0.0105$ (i.e., $\alpha=300$). However, the realization of weak-nonlinearity-based QC using homodyne detection will still be extremely hard. We set $\chi=0.01$ and consider the following two examples in Fig. 4. In the first example, $\alpha=10^3$ where the required angle is $\theta\approx 0.13$, and in the second, $\alpha=10^4$ and $\theta\approx 0.04$. Figure 4 clearly shows that the energy decay rate γ should be extremely small in the case of homodyne detection, which is not realistic using current technology.

TABLE I. The amplitude parameter $\mathcal{A}$ and coherence parameter $|\mathcal{C}|$ under various conditions. α is the initial amplitude of the probe coherent state and "Length" is the required length of the optical fiber. (a) Cases for homodyne detection with d_{HD} ($\approx\alpha\theta^2/2$)=4. Comparing $\mathcal{A}$ and $|\mathcal{C}|$, it is obvious that this detection strategy cannot be used for a weak-nonlinearity-based two-qubit parity gate. (b) Cases for photon-number-resolving detection with d_{PD} ($\approx\alpha\theta$)=π. Both $\mathcal{A}$ and $|\mathcal{C}|$ approach 1 simultaneously when α becomes large.

χ/γ	θ ($=\chi t$)	α	Length (km)	$\mathcal{A}$	$\lvert\mathcal{C}\rvert$
		(a) Homodyne detection			
0.0125	0.284	100	271	10^{-5}	0.210
	0.163	300	130	0.0014	$\sim$0
	0.052	3000	50	0.127	$\sim$0
0.0303	0.284	100	271	0.009	10^{-4}
	0.163	300	130	0.067	$\sim$0
	0.052	3000	50	0.427	$\sim$0
		(b) Photon number resolving detection			
0.0125	0.0105	300	10	0.658	0.474
	1.05×10^{-3}	3000	1	0.959	0.878
	1.05×10^{-4}	3×10^4	0.1	0.996	0.985
0.0303	0.0105	300	10	0.841	0.644
	1.05×10^{-3}	3000	1	0.983	0.946
	1.05×10^{-4}	3×10^4	0.1	0.998	$>$0.99

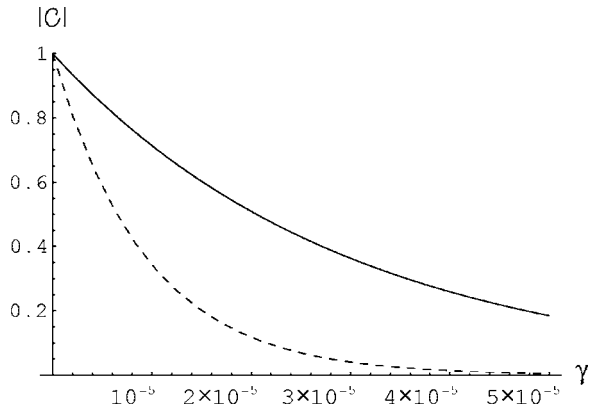

FIG. 4. The absolute coherence parameter $|\mathcal{C}|$ against the energy decay rate γ. The nonlinear strength is assumed to be $\chi=0.01$. Note that the amplitude parameter $\mathcal{A}$ will be always close to 1 in this regime since γt is very small. The solid line corresponds to $\alpha=10^3$ so that $\theta_{HD}=\chi t\approx 0.13$. The dashed line corresponds to $\alpha=10^4$ and $\theta_{HD}=\chi t\approx 0.04$. The coherence parameter $|\mathcal{C}|$ rapidly decreases for a small increase of γ.

IV. DISCUSSION

In the weak-nonlinearity-based QC scheme, a strong probe coherent field with a large amplitude is necessarily required. However, as the amplitude of the coherent field gets larger, decoherence during nonlinear interaction rapidly increases when homodyne detection is used. On the contrary, decoherence diminishes under the same conditions when photon-number-resolving measurement is used. This shows that weak-nonlinearity-based QC can naturally overcome decoherence during nonlinear interactions simply by using strong probe fields, when photon-number-resolving detection is used.

Since $d_{PD}=\pi$ in Eq. (5) is required for a small error probability, the photodetector for the two-qubit gate should be able to discriminate about ten ($\approx d_{PD}^2$) photons. Such detection ability is extremely demanding using current technology. It may be crucial to first develop the photon-number-resolving QND technique using a weak nonlinearity, a strong coherent field, and homodyne detection in Ref. [12], which was employed for the two-qubit gate in Ref. [16]. Here, we point out that the QND technique in Ref. [12] does not suffer the increase of decoherence for large probe field amplitudes in the nonlinear medium because distinguishability of this QND scheme [12] depends on $\approx\alpha\theta$, not on $\approx\alpha\theta^2$.

Using photon-number-resolving detection in the weak-nonlinearity-based two-qubit parity gate also requires a highly precise displacement operation $D(-\alpha)$, with a very large α. The displacement operation can be performed using a strong coherent field and a beam splitter with high transmittivity. It would be experimentally challenging since the average photon number of the probe coherent field should be $|\mathcal{A}^2\alpha|^2\gg 10^6$ to obtain good coherence as can be seen in Table I(b).

The two-qubit parity gate that we have considered in this paper is based on two weak nonlinearities, a probe coherent field, a probe beam measurement, and classical feedforward as shown in Fig. 1 [14–17]. Here, we note the recently suggested weak-nonlinearity-based controlled-phase gate by Spiller *et al.* [26], where the probe beam measurement is not necessary, at the cost of using additional nonlinearities and displacement operations. The requirement of successful achievement of this gate is $\alpha\theta\sim 1$ [26,27], which satisfies the condition for robustness against decoherence analyzed in this paper. Therefore, such an approach without the probe beam measurement may be considered as an alternative to the weak-nonlinearity-based parity gate in Fig. 1 using photon-number-resolving detection.

We have explained the reason for the decrease of decoherence when photon-number-resolving detection is used. Qualitatively, decoherence depends on the interaction time t and the travel path $\alpha\theta$ of the component coherent state in Fig. 2. In other words, one can expect that decoherence effects will increase when either t or $\alpha\theta$ becomes large. As the initial amplitude α of the probe beam increases, the interaction time t is reduced while $\alpha\theta$ remains approximately the same when photon-number-resolving detection is used, which causes a decrease of the decoherence effects. This is not the case for homodyne detection: in the case of homodyne detection, $\alpha\theta$ should become larger as α increases, which results in an increase of the decoherence effects.

We finally point out that certain types of errors cannot be made small in the way explained above. For example, in a real experiment, self-phase modulation (SPM) will also occur during the cross-Kerr interactions in optical fibers [28]. It may hinder measuring the phase shift purely induced by the cross-Kerr effects in weak-nonlinearity-based QC. Note that the principle of the weak-nonlinearity-based approach is to use a large-amplitude probe beam to compensate the weak strength of the nonlinearity. This mechanism is applied to both the cross-Kerr effects and the SPM effects [18]. Therefore, the ratio between the cross-Kerr effect and the SPM effect during the interaction between the probe beam and the single-photon qubit in the nonlinear medium will not be affected by the detection strategy or the initial amplitude. This kind of error should be separately dealt with (for example, see Ref. [29]).

ACKNOWLEDGMENTS

This work was supported by the Australian Research Council. The author would like to thank S. D. Barrett, T. C. Ralph, A. M. Branczyk, and W. J. Munro for valuable comments and stimulating discussions.

[1] W. H. Zurek, Phys. Today **44**(10), 36 (1991).
[2] E. Schrödinger, Naturwiss. **23**, 807 (1935); **23**, 823 (1935); **23**, 844 (1935).
[3] M. S. Kim and V. Bužek, Phys. Rev. A **46**, 4239 (1992).
[4] C. H. Bennett, D. P. DiVincenzo, J. A. Smolin, and W. K. Wootters, Phys. Rev. A **54**, 3824 (1996).
[5] B. Yurke and D. Stoler, Phys. Rev. Lett. **57**, 13 (1986).
[6] Q. A. Turchette, C. J. Hood, W. Lange, H. Mabuchi, and H. J. Kimble, Phys. Rev. Lett. **75**, 4710 (1995).
[7] M. Brune, E. Hagley, J. Dreyer, X. Maître, A. Maali, C. Wunderlich, J. M. Raimond, and S. Haroche, Phys. Rev. Lett. **77**, 4887 (1996).
[8] G. J. Milburn, Phys. Rev. Lett. **62**, 2124 (1989).
[9] J. Fiurášek, L. Mišta, Jr., and R. Filip, Phys. Rev. A **67**, 022304 (2003).
[10] H. Jeong, Ph.D. thesis, Queen's University Belfast, U.K., 2003 (unpublished).
[11] H. Jeong, Phys. Rev. A **72**, 034305 (2005).
[12] W. J. Munro, Kae Nemoto, R. G. Beausoleil, and T. P. Spiller, Phys. Rev. A **71**, 033819 (2005).
[13] S. D. Barrett, P. Kok, K. Nemoto, R. G. Beausoleil, W. J. Munro, and T. P. Spiller, Phys. Rev. A **71**, 060302(R) (2005).
[14] K. Nemoto and W. J. Munro, Phys. Rev. Lett. **93**, 250502 (2004).
[15] W. J. Munro, Kae Nemoto, T. P. Spiller, S. D. Barrett, Pieter Kok, and R. G. Beausoleil, J. Opt. B: Quantum Semiclassical

Opt. **7**, S135 (2005).
[16] W. J. Munro, K. Nemoto, and T. Spiller, New J. Phys. **7**, 137 (2005).
[17] K. Nemoto and W. J. Munro, Phys. Lett. A **344**, 104 (2005).
[18] H. Jeong, M. S. Kim, T. C. Ralph, and B. S. Ham, Phys. Rev. A **70**, 061801(R) (2004).
[19] M. S. Kim and M. Paternostro, e-print quant-ph/0510057.
[20] E. Knill, R. Laflamme, and G. J. Milburn, Nature (London) **409**, 46 (2001).
[21] C. C. Gerry, Phys. Rev. A **59**, 4095 (1999).
[22] S. J. D. Phoenix, Phys. Rev. A **41**, 5132 (1990).
[23] B. C. Sanders and G. J. Milburn, Phys. Rev. A **45**, 1919 (1992); **39**, 694 (1989).
[24] H. Kanamori, H. Yokota, G. Tanaka, M. Watanabe, Y. Ishiguro, I. Yoshida, T. Kakii, S. Itoh, Y. Asano, and S. Tanaka, J. Lightwave Technol. **4**, 1144 (1986); S. A. Bashar, in *Proceedings of the IEB Second International Conference on Electrical Engineering*, Khulna, Bangladesh, 2002 (unpublished).
[25] K. Nagayama, M. Matsui, M. Kakui, T. Saitoh, K. Kawasaki, H. Takamizawa, Y. Ooga, I. Tsuchiya, and Y. Chigusa, Technol. Rev. **57**, 3 (2004).
[26] T. P. Spiller, K. Nemoto, S. L. Braunstein, W. J. Munro, P. van Loock, and G. J. Milburn, New J. Phys. **8**, 30 (2006).
[27] W. J. Munro (private communication).
[28] G. P. Agrawal, *Nonlinear Fiber Optics*, 3rd ed. (Academic Press, San Diego, 2001).
[29] Y. Li, C. Hang, L. Ma, and G. Huang, e-print quant-ph/0511027. In this reference, the authors studied a scheme using EIT which may detach and reduce the SPM effect during cross-Kerr interactions.